Adaptive Bit Loading and Transmit Diversity for Iterative OFDM Receivers

Stephan Sand and Christian Mensing
German Aerospace Center (DLR)
Institute of Communications and Navigation
Oberpfaffenhofen, 82234 Wessling, Germany
Email: {stephan.sand, christan.mensing}@dlr.de

Carlo Mutti and Armin Wittneben
Swiss Federal Institute of Technology (ETH) Zurich
Communication Technology Laboratory
Sternwartstrasse 7, CH-8092 Zurich, Switzerland
Email: {mutti, wittneben}@nari.ee.ethz.ch

***Abstract*— In this paper, we consider a transmission system employing orthogonal frequency division multiplexing (OFDM) with bit-interleaved coded modulation and perfect channel state information at both transmitter and receiver. An adaptive bit loading scheme in combination with cyclic delay diversity and discontinuous Doppler diversity is proposed at the transmitter and iterative demapping and decoding at the receiver. The loading procedure minimizes the bit-error rate at the decoder output, and the transmit diversity schemes mitigate channel correlations. We analyze the iterative receiver with extrinsic information transfer charts and present the achievable gains.**

I. Introduction

Orthogonal frequency-division multiplexing (OFDM) in combination with bit-interleaved coded modulation (BICM) has turned out a robust yet implementation efficient technique for reliable communication over fading channels without channel state information (CSI) at the transmitter [1]. If the transmitter has CSI, e.g., obtained by exploiting channel reciprocity in time-division duplex systems, the negative effects of the fading can be further alleviated by an adaptation of the signaling to the varying channel gain [2], [3].

Water-filling based adaptive bit loading (ABL) schemes are well-known in the field of transmission over twisted-pair lines [4]. Since practical wireless systems, however, usually operate far from the theoretical capacity, adaptation techniques should have a different optimization criterion. If we assume that the transmitter has perfect CSI, adaptive techniques to improve the average bit-error rate (BER) performance in environments with frequency-selective fading are proposed in [5]. In general, this can only be achieved in low mobility scenarios where the channel is changing slowly. For such channels, a typical environment could be a small office or conference room [6], where the user is moving slowly [7]. However, this scenario may not offer high frequency-selectivity as we will show in this paper, and ABL provides only a marginal gain w.r.t. uniform bit loading (UBL).

Dammann [8] introduced cyclic delay diversity (CDD) to increase the frequency-selectivity by sending multiple cyclically delayed copies of the original transmit signal over several transmit antennas. The advantages of CDD are that it causes no inter-symbol interference (ISI) and a one antenna receiver is sufficient to recover the transmit signal. Compared to orthogonal space-time block codes, CDD needs no additional processing at the receiver and it can employ an arbitrary number of transmit antennas as a rate one space-time code [9]. Thus, ABL together with CDD can yield significant performance gains compared to UBL. In addition, we can employ discontinuous Doppler diversity (DDoD) [10] to increase the time diversity.

At the receiver, the system performance can be further improved by iteratively exchanging extrinsic information between the demapper and decoder [11]. The critical design parameter for a BICM receiver with iterative demapping and iterative decoding (IDEM) is the choice of the symbol alphabet mapping, i.e., the labeling map between the bits and the symbol alphabet elements. To predict and analyze the performance of IDEM, extrinsic information transfer (EXIT) charts are a well established tool [11]–[14].

In this paper, we study the effect of correlated channels for an ABL scheme in a BICM-OFDM system with IDEM. We show that the ABL scheme can be easily combined with the transmit diversity techniques CDD and DDoD to compensate the time- and frequency correlations of the channel. Furthermore, we analyze the EXIT charts of the ABL scheme in combination with the promising IDEM scheme [12] for different mappings. Finally, BER simulations verify the performance gains predicted by the EXIT charts.

II. System Model

We consider the coded OFDM transmission set-up sketched in Figures 1 and 2. According to the principle of BICM, a bit-wise interleaving (π) is performed after convolutional encoding. The coded bits c_μ, where μ denotes the bit index in the codeword, are mapped by the ABL module onto N_c subcarriers and N_s OFDM symbols forming the OFDM frame $S_{n,k}$ for $n = 0, \ldots, N_\mathrm{c}-1$ and $k = 0, \ldots, N_\mathrm{s}-1$. Let $v_{n,k}$ denote the number of coded bits associated with the n-th subcarrier of the k-th OFDM symbol. We restrict the possible signal sets to have square lattice signal constellations, i.e., we consider 4-, 16-, and 64-quadrature amplitude modulation (QAM). The extension to higher order alphabets is straightforward. In any case, the coded bits are assumed uniformly distributed and independent due to the preceding ideal interleaving.

The main task of the ABL module is the selection of the values $v_{n,k}$ on the basis of the given CSI. The choice of $v_{n,k}$ is subject to the bit-rate constraint

$$\sum_{n=0}^{N_\mathrm{c}-1} \sum_{k=0}^{N_\mathrm{s}-1} v_{n,k} = V_\mathrm{B}, \qquad v_{n,k} \in \{2, 4, 6\}, \tag{1}$$

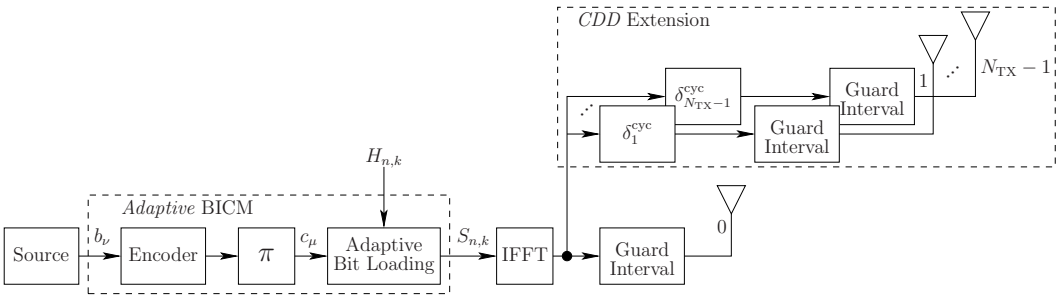

Fig. 1. BICM-OFDM transmitter with ABL and CDD extension.

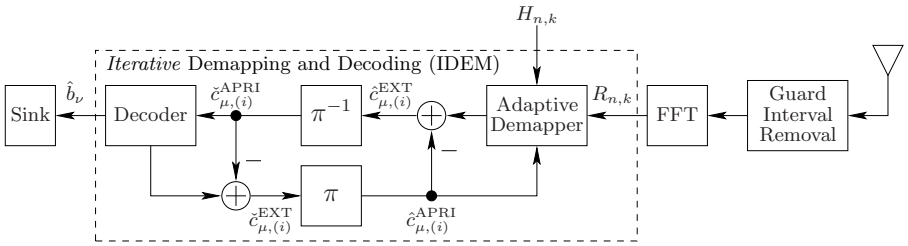

Fig. 2. Iterative BICM-OFDM receiver.

where V_{B} denotes the total number of bits per OFDM frame. Each OFDM symbol is transformed by an inverse fast Fourier transform (IFFT) of size N_{FFT} in the time domain, and cyclically extended by the guard interval before it is transmitted over a time-variant multipath channel. When employing the CDD extension at the transmitter, the time domain signal after the IFFT is cyclicly delayed for each additional transmit antenna by δ^{cyc}_m, where $m = 1, \ldots, N_{\text{TX}} - 1$ (cf. Section IV). In this case, the OFDM signal is normalized by $1/\sqrt{N_{\text{TX}}}$ to keep the average transmit power independent of the number of transmit antennas N_{TX}. In addition to CDD, the transmitter can utilize DDoD (cf. Section IV).

At the receiver, zero-mean additive white Gaussian noise (AWGN) results in a corruption of the signals at the FFT output by independent complex Gaussian noise terms with variance N_0. The adaptive demapper computes from the received symbols $R_{n,k}$ soft-demodulated extrinsic log-likelihood ratio values $\hat{c}^{\text{EXT}}_{\mu,(i)}$ (L-values [12]), where (i) denotes the iteration index. To obtain the L-values, the adaptive demapper uses the a-priori L-values $\check{c}^{\text{APRI}}_{\mu,(i)}$ coming from the decoder and the channel coefficients $H_{n,k}$. In the initial iteration ($i = 0$), the demapper assumes that the L-values $\check{c}^{\text{APRI}}_{\mu,(i)}$ are zero. Note, in this paper we assume perfect CSI. In a practical receiver, however, the CSI has to be estimated [14]. After deinterleaving (π^{-1}), the extrinsic L-values $\hat{c}^{\text{EXT}}_{\mu,(i)}$ become the a-priori L-values to the channel decoder. The channel decoder computes for all code bits the L-values $\check{c}^{\text{EXT}}_{\mu,(i)}$ using the maximum a-posteriori (MAP) algorithm. The extrinsic L-values are then interleaved to become the a-priori L-values $\hat{c}^{APRI}_{\mu,(i)}$ used in the next iteration in the demapper.

In the i-th iteration ($i > 0$), the newly obtained a-priori L-values $\hat{c}^{APRI}_{\mu,(i)}$ are fed back to the demapper to improve the estimated extrinsic L-values $\hat{c}^{\text{EXT}}_{\mu,(i)}$. The above described iterative demapping and decoding can be repeated several times. In the final iteration, the decoder returns hard decision estimates $\hat{b}_\nu$ of the transmitted bits using the MAP algorithm.

III. Adaptive Bit Loading

In the sequel, we analyze ABL for Gray mapping [15] only. As a consequence of the ideal interleaving, the superchannel constituted by all the entities in Figures 1 and 2 from the interleaver at the transmitter up to the deinterleaver at the receiver may be viewed as a memoryless binary symmetric channel (BSC) with a certain transition probability. Adopting the equivalent channel model introduced for a BICM system in [1], the exact uncoded bit-error probability (UBEP) can be computed for each of the parallel independent binary input channels. This can be done by first expressing the probabilities of a corresponding bit-error event conditioned on each of the QAM signals in both quadrature components, and then averaging over these conditional probabilities.

For a given channel realization, the UBEP for the n-th subcarrier of the k-th OFDM symbol after the demapper for a 4-QAM signal set is given as

$$P^{(n,k)}_{\text{b,4-QAM}} = \text{Q}\big(\sqrt{\gamma_{n,k}}\big), \tag{2}$$

where $\gamma_{n,k}$ denotes the signal-to-noise ratio (SNR) for the n-th subcarrier of the k-th OFDM symbol. The corresponding formulas for 16-QAM and 64-QAM are [16]

$$P^{(n,k)}_{\text{b,16-QAM}} = \frac{3}{4}\text{Q}\left(\sqrt{\frac{\gamma_{n,k}}{5}}\right) + \frac{1}{2}\text{Q}\left(\sqrt{\frac{9\gamma_{n,k}}{5}}\right) - \frac{1}{4}\text{Q}\big(\sqrt{5\gamma_{n,k}}\big) \tag{3}$$

and

$$P^{(n,k)}_{\text{b,64-QAM}} = \frac{7}{12}\text{Q}\left(\sqrt{\frac{\gamma_{n,k}}{21}}\right) + \frac{1}{2}\text{Q}\left(\sqrt{\frac{3\gamma_{n,k}}{7}}\right) + \frac{1}{12}\text{Q}\left(\sqrt{\frac{27\gamma_{n,k}}{7}}\right) - \frac{1}{12}\text{Q}\left(\sqrt{\frac{25\gamma_{n,k}}{21}}\right) - \frac{1}{12}\text{Q}\left(\sqrt{\frac{169\gamma_{n,k}}{21}}\right), \tag{4}$$

respectively. The average UBEP is given as

$$P_{\mathrm{b}} = \frac{1}{V_{\mathrm{B}}}\Bigg(\sum_{(n,k)\in\Omega_{4\text{–QAM}}} 2P_{\mathrm{b,4\text{–QAM}}}^{(n,k)} + \sum_{(n,k)\in\Omega_{16\text{–QAM}}} 4P_{\mathrm{b,16\text{–QAM}}}^{(n,k)} + \sum_{(n,k)\in\Omega_{64\text{–QAM}}} 6P_{\mathrm{b,64\text{–QAM}}}^{(n,k)} \Bigg), \tag{5}$$

where V_{B} is kept constant over the OFDM frame, and $\Omega_{4\text{–QAM}}, \Omega_{16\text{–QAM}}, \Omega_{64\text{–QAM}}$ are the set of subcarrier indices n,k for the different modulation alphabets such that the $\mathrm{card}(\Omega_{4\text{–QAM}} \cup \Omega_{16\text{–QAM}} \cup \Omega_{64\text{–QAM}}) = N_{\mathrm{c}}N_{\mathrm{s}} = N_{\mathrm{B}}$ with $\mathrm{card}(\cdot)$ denoting cardinality. In general, it is difficult to derive exact BEP expressions for coded systems. However, for a BICM-OFDM system, the exact BEP can be upper bounded using the pairwise error probability (PEP) [1]. Here, we prefer to have an exact UBEP for the ABL scheme rather than using the PEP analysis to derive the loading scheme.

Since the BER of a coded transmission over a memoryless BSC decreases with the transition probability of the channel, the subsequent loading procedure is based on a minimization of P_{b} in (5) w.r.t. $v_{n,k}$ subject to the constraint in (1). In [17], it has been shown that the integer constraint of $v_{n,k}$ can be easily taken into account using the Lagrange multiplier method. However, this discrete bit allocation problem cannot, in general, be solved explicitly but requires an iterative solution. The iterative process involves repeatedly the minimization of the overall UBEP w.r.t. the values $v_{n,k}$ while keeping V_{B} constant.

The dependence of P_{b} on the values $v_{n,k}$ has been investigated in [17] for the case of a system with $N_{\mathrm{B}} = 2$. The direct minimization of the UBEP as in [17] is excluded for the general case $N_{\mathrm{B}} > 2$, since the UBEP expressions are complicated functions of the modulation alphabets, subcarrier SNR values as well as the overall SNR.

Instead of carrying out an exhaustive search as described in [5], we can devise a heuristic iterative approach based on the considerations for $N_{\mathrm{B}}=2$. We assume an even N_{B}, where the extension to an odd N_{B} is straightforward. The objective is to devise a simple algorithm which leads to a monotonically decreasing UBEP as a function of the iteration index. However, the final UBEP might not be the minimum one. The algorithm can be formulated as follows:

1) Sort the power channel coefficients $|H_{0,0}|^2, \ldots, |H_{N_{\mathrm{c}}-1,N_{\mathrm{s}}-1}|^2$ in increasing order and assign the indices of the channel coefficients upon sorting to $\kappa_1, \ldots, \kappa_{N_{\mathrm{B}}}$.
2) Taking into account the bit-rate constraint in (1) with $V_{\mathrm{B}}=4N_{\mathrm{B}}$, we consider the $N_{\mathrm{B}}/2+1$ possible modes $\mathbf{m}$ for the sorted channel according to Table I.
3) Start with mode $\mathbf{m}_1$ and calculate the resulting UBEP.
4) In each iteration step, increase the mode index by one, calculate the UBEP for the new mode, continue until the newly calculated UBEP is larger than the previous UBEP and finally choose the previous mode index.

IV. Cyclic Delay Diversity and Discontinuous Doppler Diversity

In the previous section, we assumed that the channel fading coefficients $H_{n,k}$ between adjacent subcarriers are uncorrelated. However, in any practical OFDM system, we will have correlations between neighboring subcarriers. The bandwidth over that adjacent subcarriers are correlated is the coherence bandwidth $(\Delta f)_{\mathrm{c}}$ of the channel, which can be approximated as $(\Delta f)_{\mathrm{c}} \approx 1/\tau_{\max}$ [18] with $\tau_{\max}$ denoting the maximum channel delay. As a conservative estimate, the guard interval is larger than the the maximum channel delay $\tau_{\max}$ and synchronization errors, i.e., $T_{\mathrm{GI}} > \tau_{\max}$. Thus, the coherence bandwidth is lower bounded by $1/T_{\mathrm{GI}} = \frac{N_{\mathrm{FFT}}}{N_{\mathrm{GI}}}F_{\mathrm{s}}$, where F_{s} denotes the subcarrier spacing and N_{GI} the guard interval length. For instance, the coherence bandwidth $(\Delta f)_{\mathrm{c}}$ is greater than 4 to 50 subcarriers if $N_{\mathrm{GI}} \in [N_{\mathrm{FFT}}/50, \ldots, N_{\mathrm{FFT}}/4]$. Usually, $\tau_{\max}$ is much smaller than T_{GI} resulting in an even larger coherence bandwidth and more correlated subcarriers. Consequently, ABL may not yield significant performance gains compared to UBL to justify the additional complexity.

TABLE I
POSSIBLE MODES FOR AN EVEN N_{B}.

mode \ subcarrier	κ_1	κ_2	κ_3	$\cdots$	$\kappa_{\frac{N_{\mathrm{B}}}{2}}$	$\kappa_{\frac{N_{\mathrm{B}}}{2}+1}$	$\cdots$	$\kappa_{N_{\mathrm{B}}-1}$	$\kappa_{N_{\mathrm{B}}}$
$\mathbf{m}_1$	4	4	4	$\cdots$	4	4	$\cdots$	4	4
$\mathbf{m}_2$	2	4	4	$\cdots$	4	4	$\cdots$	4	6
$\mathbf{m}_3$	2	2	4	$\cdots$	4	4	$\cdots$	6	6
$\vdots$	$\vdots$	$\vdots$	$\vdots$	$\vdots$	$\vdots$	$\vdots$	$\vdots$	$\vdots$	$\vdots$
$\mathbf{m}_{N_{\mathrm{B}}/2}$	2	2	2	$\cdots$	4	4	$\cdots$	6	6
$\mathbf{m}_{N_{\mathrm{B}}/2+1}$	2	2	2	$\cdots$	2	6	$\cdots$	6	6

To reduce the frequency correlations, we apply CDD to the OFDM system as described in detail in [8]. After the IFFT the time domain signal $s_{u,k}$ is given by

$$s_{u,k} = \frac{1}{\sqrt{N_{\mathrm{FFT}}}} \sum_{n=0}^{N_{\mathrm{FFT}}-1} S_{n,k} e^{j\frac{2\pi}{N_{\mathrm{FFT}}}nu}, \tag{6}$$

where u denotes the chip time index of the k-th OFDM symbol. The CDD transmit signal for antenna m is then equal to

$$s_{u,k}^{m} = \frac{1}{\sqrt{N_{\mathrm{TX}}}} s_{((u-\delta_m^{\mathrm{cyc}}) \bmod N_{\mathrm{FFT}}),k}, \tag{7}$$

where $x \bmod y$ is the modulo operator returning the remainder of the division of x by y. Transforming $s_{u,k}^{m}$ back into the frequency domain, we obtain

$$S_{n,k}^{m} = \frac{1}{\sqrt{N_{\mathrm{TX}}}} S_{n,k} e^{-j\frac{2\pi}{N_{\mathrm{FFT}}}\delta_m^{\mathrm{cyc}}n}. \tag{8}$$

Consequently, the received signal $R_{n,k}$ is given by

$$\begin{aligned} R_{n,k} &= \frac{1}{\sqrt{N_{\mathrm{TX}}}} S_{n,k} \sum_{m=0}^{N_{\mathrm{TX}}-1} H_{n,k}^{m} e^{-j\frac{2\pi}{N_{\mathrm{FFT}}}\delta_m^{\mathrm{cyc}}n} + Z_{n,k} \\ &= S_{n,k} H_{n,k}^{\mathrm{CDD}} + Z_{n,k}, \end{aligned} \tag{9}$$

where $H_{n,k}^{m}$ is the channel transfer function (CTF) between transmit antenna m and the receive antenna, $H_{n,k}^{\mathrm{CDD}}$ the equivalent CTF experienced by the receiver, and $Z_{n,k}$ AWGN.

From (9), we infer that CDD causes no ISI although the cyclic delays δ_m^{cyc} may be larger than the guard interval. Further, CDD does not require any additional signal processing at the receiver and hence, is a standard conformable antenna diversity technique [8]. The spatial diversity of the transmit

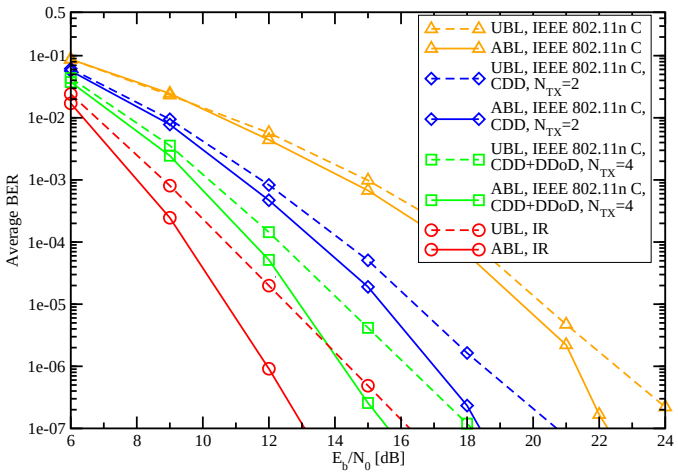

Fig. 3. Average BER values for a BICM-OFDM system applying ABL, UBL, and transmit diversity techniques over different channels.

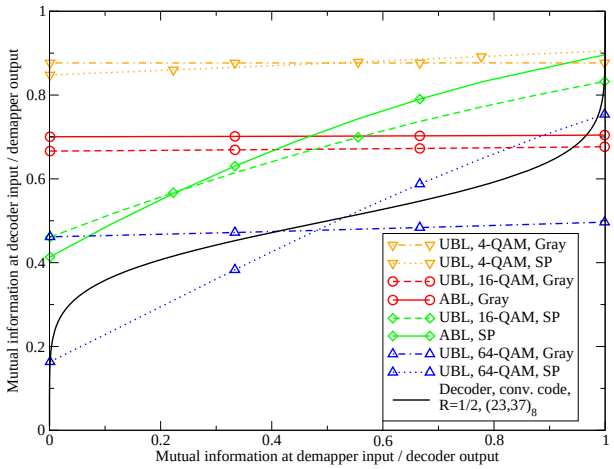

Fig. 4. EXIT chart of ABL and UBL schemes for an iterative BICM-OFDM receiver at 10.5 dB $\mathrm{E_s/N_0}$, which corresponds to 7.5 dB $\mathrm{E_b/N_0}$ for 16-QAM and rate $R = 1/2$ code.

antennas is transformed into the equivalent $H_{n,k}^{\mathrm{CDD}}$ with increased frequency diversity. For a large number of uncorrelated transmit antennas, the channel fading coefficients $H_{n,k}^{\mathrm{CDD}}$ between neighboring subcarriers become uncorrelated. Thus, the ABL algorithm together with CDD can yield significant performance gains compared to UBL.

In addition it is possible to increase the time diversity with DDoD without causing inter-carrier interference (ICI) [10]. In that case, the time domain signal for antenna m becomes

$$s_{u,k}^{m} = \frac{1}{\sqrt{N_{\mathrm{TX}}}} s_{u,k} \cdot e^{j\frac{2\pi(N_{\mathrm{FFT}}+N_{\mathrm{GI}})}{N_{\mathrm{FFT}}} T_{\mathrm{s}} \Delta f_m k}, \qquad (10)$$

where $T_{\mathrm{s}} = 1/F_{\mathrm{s}}$ denotes the OFDM symbol duration and Δf_m the antenna specific spectrum shift. Note that we can combine both CDD and DDoD to increase diversity.

V. Simulation Results

In this section, we investigate the achievable performance gains resulting from the schemes in Section III and IV with perfect CSI at the transmitter and receiver.

To obtain BER simulation results for the ABL procedure of Section III, we consider a small office environment as simulation scenario, i.e., the 802.11n C channel model [7] with non-line-of-sight propagation, $\tau_{\max} = 200\mathrm{ns}$, and bell shaped Doppler power spectrum (maximum Doppler frequency $f_{\mathrm{D,max}} \approx 29$ Hz at the carrier frequency $f_{\mathrm{c}} = 5.25$ GHz). A BICM-OFDM scheme is assumed employing a rate $R = 1/2$ convolutional code with generators $(23, 37)_8$ [12], $N_{\mathrm{c}} = 990$ active subcarriers with $F_{\mathrm{s}} = 20$ kHz occupying a bandwidth of 19.8 MHz. The resulting OFDM symbol duration is $T_{\mathrm{s}} = 50\mu\mathrm{s}$ and the sampling time $T_{\mathrm{samp}} = T_{\mathrm{s}}/N_{\mathrm{FFT}} = 48.828\mathrm{ns}$, where $N_{\mathrm{FFT}} = 1024$. We choose a guard interval $T_{\mathrm{GI}} = 21 T_{\mathrm{samp}} \approx 1.03\mu\mathrm{s}$. The system transmits $N_{\mathrm{s}} = 101$ OFDM symbols per frame resulting in a frame duration of $5.15\mathrm{ms}$ and a data rate of $38.8\mathrm{Mbps}$.

Figure 3 displays the average BERs at the decoder output as a function of the SNR $\mathrm{E_b/N_0}$ for ABL and UBL using Gray mapping. Since Gray mapping does not benefit from IDEM [12], a non-iterative receiver estimates the transmitted bits. For an average BER of 10^{-6} and a system without CDD and DDoD, we observe an SNR gain of about 1.2 dB for the ABL as compared to the UBL. This relative gain increases by using CDD and CDD+DDoD. For $N_{\mathrm{TX}} = 4$, we create two pairs of antennas, where within each pair the second transmit signal is cyclically delayed by $\delta_1^{\mathrm{cyc}} = 10\, T_{\mathrm{samp}}$. The first pair experiences a discontinuous Doppler shift of $\Delta f_0 = -583$ Hz and the second one a shift of $\Delta f_1 = 583$ Hz (cf. (10)). The results indicate also that for increasing the number of transmit antennas with CDD+DDoD, we approach the lower bounds given by ABL and UBL over an independent Rayleigh (IR) fading channel. Clearly, as the subcarriers are less correlated, ABL exhibits an increasing performance gain compared to UBL, as more independent optimization choices become available. For an IR fading channel, ABL outperforms UBL by 2.5 dB at an average BER of 10^{-6}. The SNR penalty for joint CDD and DDoD with 4 transmit antennas is about 2.25 dB and 1.78 dB for ABL and UBL, respectively.

In the following, we assume that the equivalent CTF at the receiver (9) is an IR fading channel generated by using CDD and DDoD. Now, we investigate the performance of an iterative BICM-OFDM receiver for ABL and UBL with Gray and set partitioning (SP) mapping [19]. In Figure 4, we plotted the EXIT chart for various demappers and the convolutional decoder at an $\mathrm{E_s/N_0} = 10.5$ dB, which corresponds to an $\mathrm{E_b/N_0} = \mathrm{E_s/N_0} - 10\log_{10}(R \cdot V_{\mathrm{B}}/N_{\mathrm{B}}) = 7.5$ dB for 16-QAM and $R = 1/2$. Besides the UBL curves for 16-QAM, we also plotted the UBL curves for 4- and 64-QAM as additional references. As expected for Gray mapping [12], both ABL and UBL demapper characteristics do not improve performance with additional a-priori information. Since ABL optimizes the UBEP for Gray mapping and thus the mutual information (MI) at the output of the demapper [14], it is always above the UBL curve. However, using the SP mapping, we notice that now ABL performs worse than UBL at low a-priori MI at the demapper input, intersects with UBL at approximately an MI of 0.24 and outperforms UBL at high a-priori MI. As we are only aware of exact UBEPs for Gray mapping, we used for SP

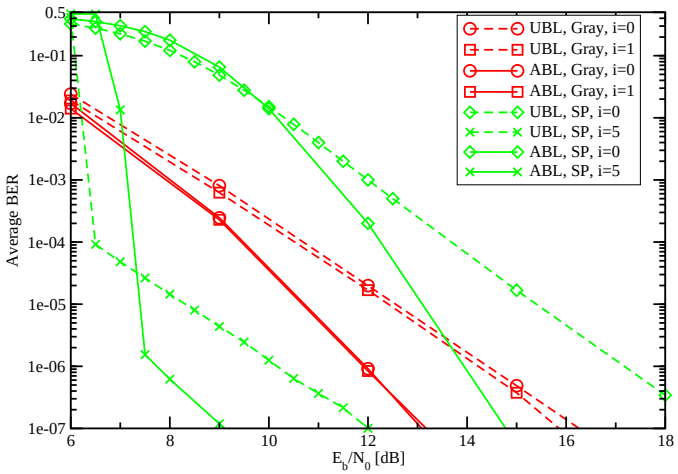

Fig. 5. Average BER values for a BICM-OFDM system with iterative receiver applying ABL and UBL with Gray and SP mappings for different iterations (i=0,1,5).

as an approximation the same UBEPs as for Gray mapping in the ABL algorithm (cf. Section III). Comparing the 4-, 16-, and 64-QAM UBL curves for Gray and SP mapping, we can see that the MI at the demapper output of SP is always worse than the one of Gray mapping at low a-priori MI and outperforms the one of Gray mapping at high a-priori MI. According to [13], [14], we can map the MI at the demapper output to an average UBEP, where for increasing MI, the UBEP decreases. Since at low a-priori MI, the MI at the demapper output for SP is always worse than the one for Gray mapping, the UBEP for SP will be larger than the one for Gray mapping. However, at high a-priori MI, the MI at the demapper output for SP is always better than the one for Gray mapping and hence, the UBEP for SP will be smaller than the one for Gray mapping. Therefore, the approximation for SP in the ABL algorithm calculates too small UBEPs at low a-priori MI and too large UBEPs at high a-priori MI. Consequently, UBL with SP outperforms ABL with SP at low a-priori MI, and ABL with SP can outperform UBL only at medium to high a-priori MI, which is in contrast to Gray mapping. Considering high a-priori MI, both ABL and UBL for Gray mapping should result in a large BER at $\mathrm{E_b/N_0} = 7.5$ dB, whereas ABL and UBL with SP should result in a significant lower BER. Further, at $\mathrm{E_s/N_0} = 10.5$ dB ABL with SP and an average of 4 bits per symbol performs as well as UBL for 4-QAM and SP. Hence, we expect the same BER for ABL with SP at 3 dB less $\mathrm{E_b/N_0}$ and twice the spectral efficiency.

Figure 5 shows the average BERs for a BICM-OFDM system with iterative receiver applying ABL and UBL for different iterations i. Note, the iterative receiver converges within five and one iterations for SP and Gray mapping. The results confirm the behavior of ABL and UBL with SP and Gray mapping predicted by the EXIT chart at 7.5 dB. At an average BER of 10^{-6}, ABL with SP outperforms UBL with SP and UBL with Gray mapping by about 2.5 dB and 6.6 dB, respectively. Using the SP mapping instead of Gray mapping in the ABL scheme results in a performance gain of 4.2 dB.

VI. Conclusions

In this article we investigate a BICM-OFDM system with ABL, CDD and DDoD schemes at the transmitter, and an IDEM scheme at the receiver. We show that CDD and DDoD can be used to achieve independent Rayleigh fading channels, and can be combined with the proposed ABL scheme without increasing its complexity or the receiver complexity. We also analyze the combination of the loading procedure with the IDEM scheme. At an average BER of 10^{-6}, it turns out that the ABL scheme with SP mapping yields a performance gain of about 6.6 dB w.r.t. UBL with Gray mapping. Here, the choice of the mapping is crucial, and further investigations are needed to adapt the ABL scheme to non Gray mappings.

References

[1] G. Caire, G. Taricco, and E. Biglieri, "Bit-interleaved coded modulation," *IEEE Trans. Inform. Theory*, vol. 44, no. 3, pp. 927–946, May 1998.

[2] T. Keller and L. Hanzo, "Adaptive modulation techniques for duplex OFDM transmission," *IEEE Trans. Veh. Technol.*, vol. 49, no. 5, pp. 1893–1906, Sept. 2000.

[3] C. Mutti, D. Dahlhaus, and T. Hunziker, "Optimal power loading for multiple-input single-output OFDM systems with bit-level interleaving," *IEEE Trans. Wireless Commun.*, pp. 1886–1895, July 2006.

[4] P. S. Chow, J. M. Cioffi, and J. A. C. Bingham, "A practical discrete multitone transceiver loading algorithm for data transmission over spectrally shaped channels," *IEEE Trans. Commun.*, vol. 43, no. 2/3/4, pp. 773–775, Feb./Mar./Apr. 1995.

[5] C. Mutti, *Link Adaptation Schemes for Wireless Multicarrier Transmission Systems*. Hartung-Gorre Verlag, 2005.

[6] 802.11n Task Group, "Usage models," IEEE P802.11, Tech. Rep. 802.11-03 802r15, Mar. 2004.

[7] ——, "TGn channel models," IEEE P802.11, Tech. Rep. 802.11-03 940r2, Jan. 2004.

[8] A. Dammann and S. Kaiser, "Transmit/receive antenna diversity techniques for OFDM systems," *European Transactions on Telecommunications*, vol. 13, no. 5, pp. 531–538, Sept.–Oct. 2002.

[9] A. Dammann, R. Raulefs, G. Auer, and G. Bauch, "Comparison of space-time block coding and cyclic delay diversity for a broadband mobile radio air interface," in *Proceedings* 6^{th} *International Symposium on Wireless Personal Multimedia Communications (WPMC 2003), Yokosuka, Japan*, vol. 2, Oct. 2003, pp. 411–415.

[10] A. Dammann and R. Raulefs, "Increasing time domain diversity in OFDM systems," in *Proceedings IEEE Global Telecommunications Conference (GLOBECOM 2004), Dallas, TX, USA*, vol. 2, Nov.–Dec. 2004, pp. 809–812.

[11] F. Schreckenbach and G. Bauch, "Bit-interleaved coded irregular modulation," *European Transactions on Telecommunications*, vol. 17, pp. 269–282, Mar. 2006.

[12] S. ten Brink, "Designing iterative decoding schemes with the extrinsic information transfer chart," *AEÜ International Journal of Electronics Communications*, vol. 54, no. 6, pp. 389–398, Dec. 2000.

[13] J. Hagenauer, "The EXIT chart," in *Proceedings 12th European Signal Processing Conference (EUSIPCO 2004), Vienna, Austria*, Sept. 2004.

[14] S. Sand, C. Mensing, and A. Dammann, "Transfer chart analysis of iterative OFDM receivers with data aided channel estimation," in *Proceedings* 3^{rd} *COST289 Workshop - Enabling Technologies for B3G Systems, Aveiro, Portugal*, July 2006.

[15] J. G. Proakis, *Digital Communications*, 3rd ed. McGraw-Hill, 1995.

[16] M. P. Fitz and J. P. Seymour, "On the Bit Error Probability of QAM Modulation," *International Journal of Wireless Information Networks*, vol. 1, no. 2, pp. 131–139, Apr. 1994.

[17] C. Mutti, D. Dahlhaus, T. Hunziker, and M. Foresti, "Bit and power loading procedures for OFDM systems with bit-interleaved coded modulation," in *IEEE Int. Conf. on Telecommunications (ICT) 2003*, Papeete, French Polynesia, Feb. 2003, pp. 1422–1427.

[18] K. Fazel and S. Kaiser, *Multi-Carrier and Spread Spectrum Systems*. John Wiley and Sons, 2003.

[19] G. Ungerboeck, "Channel coding wiht multilevel/phase signals," *IEEE Trans. Inform. Theory*, vol. IT-28, no. 1, pp. 55–67, Jan. 1982.